Full Paper

Tacrine–Flurbiprofen Hybrids as Multifunctional Drug Candidates for the Treatment of Alzheimer's Disease

Yao Chen[1,2,3], Jianfei Sun[4], Sixun Peng[1,2], Hong Liao[4], Yihua Zhang[1,2], and Jochen Lehmann[3]

[1] State Key Laboratory of Natural Medicines, China Pharmaceutical University, Nanjing, P. R. China
[2] Center of Drug Discovery, China Pharmaceutical University, Nanjing, P. R. China
[3] Lehrstuhl für Pharmazeutische/Medizinische Chemie, Institut für Pharmazie, Friedrich-Schiller-Universität Jena, Jena, Germany
[4] Neurobiology Lab, New Drug Screening Center, China Pharmaceutical University, Nanjing, P. R. China

Five tacrine–flurbiprofen hybrid compounds (**3a–e**) were synthesized as multi-target-directed compounds for the treatment of Alzheimer's disease. Compared to tacrine, two compounds (**3d** and **3e**) showed better acetylcholinesterase (AChE) inhibitory activity and others (**3b–e**) better or the same butyrylcholinesterase (BuChE) inhibitory activity. Notably, **3d** showed a mixed-type inhibitory action for AChE, indicating a "dual-binding site action" of both toward the catalytic active site (CAS) and the peripheral anionic site (PAS), whereas for BuChE, a competitive inhibitory action was observed. Furthermore, a cell-based assay on amyloid-β inhibition demonstrated that the selected target compound **3d** effectively inhibits the formation of amyloid-β *in vitro*.

Keywords: Alzheimer's disease / Amyloid-β / Cholinesterase inhibitor / Flurbiprofen / Tacrine

Received: February 27, 2013; Revised: August 14, 2013; Accepted: August 15, 2013

DOI 10.1002/ardp.201300074

Additional supporting information may be found in the online version of this article at the publisher's web-site.

Introduction

Alzheimer's disease (AD), the most common form of dementia, is characterized by loss of memory and progressive cognitive impairment [1]. Many factors are involved in the complicated pathogenesis, such as cholinergic dysfunction, deposits of amyloid-β (Aβ) and τ-protein, oxidative stress, and poor blood supply in the brain [2]. To date, the cholinergic strategy is the most common and effective therapeutic approach for the treatment of AD. It asserts that cholinesterase (ChE) inhibitors, aiming to increase the acetylcholine (ACh) level in the brain, can reduce the cognitive deficit in AD [3]. Therefore, acetylcholinesterase (AChE) and butyrylcholinesterase (BuChE), two types of enzymes responsible for hydrolyzing ACh, are therapeutic targets [4], and inhibitors of both, such as tacrine (Fig. 1) and rivastigmine, have been clinically applied.

In addition to the cholinergic strategy, the Aβ hypothesis has been widely accepted [5]. This asserts that the accumulation and aggregation of Aβ, 40/42 amino acid peptides, which are generated by the "amyloidogenic" proteolysis of the β-amyloid precursor protein (APP), catalyzed by β- and γ-secretase, is the trigger for progression of AD [6]. As a consequence, inhibiting the generation of Aβ could be beneficial for the treatment of AD. Flurbiprofen (Fig. 1) has been used as a non-steroidal anti-inflammatory drug (NSAID) and was then identified with the ability to lower Aβ40/42 peptide production by an allosteric modulation of presenilin-1 (PS-1), the major component of the γ-secretase complex [7].

A strategy named multi-target-directed ligands (MTDLs) has been widely applied in the research of novel anti-AD drugs, due to the limited and transient benefits of the traditional approach of single-target-molecule [8]. In this strategy, hybrid compounds composed of two distinct parts with different biological activities have been proved to exhibit multifunctional activities [9, 10].

Correspondence: Prof. Jochen Lehmann, Lehrstuhl für Pharmazeutische/Medizinische Chemie, Institut für Pharmazie, Friedrich-Schiller-Universität Jena, Philosophenweg 14, D-07743 Jena, Germany.
E-mail: j.lehmann@uni-jena.de
Fax: +49 3641949802

Additional correspondence: Hong Liao, E-mail: hliao@cup.edu.en; Prof. Yihua Zhang, E-mail: zyhtgd@hotmail.com

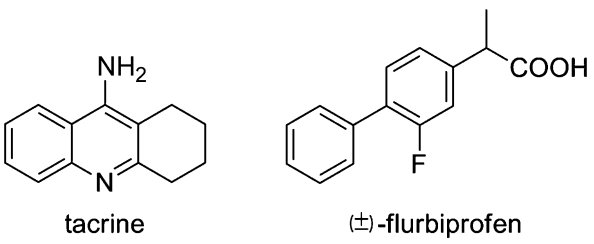

Figure 1. Structures of tacrine and flurbiprofen.

In this study, a series of tacrine–flurbiprofen hybrids (**3a–e**), in which the tacrine-like heterocycle was connected to racemic flurbiprofen via alkylenediamine linkers, were designed and synthesized, in order to achieve potential multi-potent anti-AD drugs.

Results and discussion

The intermediate 9-chloro-1,2,3,4-tetrahydroacridine **1** was synthesized according to a previously reported protocol [11] using anthranilic acid and cyclohexanone as starting materials. Then different alkylenediamines were introduced to **1** to give the 9-aminoalkylamino-1,2,3,4-tetrahydroacridines **2a–e**, which were finally connected to racemic flurbiprofen in the presence of DCC/DMAP, yielding the target compounds **3a–e** (Scheme 1).

Target compounds **3a–e** were evaluated *in vitro* as inhibitors of the AChE from *Electrophorus electricus* (eeAChE) and of the BuChE from equine serum, following Ellman's method [12] (Table 1). Among them, **3d** and **3e** showed better inhibitory activity for AChE than tacrine. For BuChE, all compounds exhibited the same or better inhibitory activity compared to tacrine with the exception of **3a**. Interestingly, the results revealed that the length of the diamine side chain might influence the ability to inhibit ChE. Compounds **3d** and **3e** showed high activity toward both AChE and BuChE (IC_{50} of AChE = 19.3 and 34.5 nM; IC_{50} of BuChE = 3.7 and 2.1 nM), which suggests the optimal spacer length to be six atoms. Notably, compound **3b** showed much higher activity toward BuChE (IC_{50} = 13.9 nM) than AChE (IC_{50} = 344.8 nM), demonstrating **3b** as a selective BuChE inhibitor (selectivity ratio = 24.8).

Table 1. Inhibition of AChE and BuChE (IC_{50} values) and selectivity expressed as the ratio of the resulting IC_{50} values.

Compd.	IC_{50} (nM) ± SEM[a)]		Selectivity ratio[b)]
	AChE	BChE	
Tacrine	61.7 ± 14.9	9.0 ± 1.8	6.9
3a	714.9 ± 251.7	58.7 ± 7.3	12.2
3b	344.8 ± 45.5	13.9 ± 3.4	24.8
3c	193.1 ± 8.5	11.0 ± 1.6	17.6
3d	19.3 ± 3.4	3.7 ± 0.4	5.2
3e	34.5 ± 3.3	2.1 ± 0.3	16.4

[a)] Data are the mean of at least three determinations.
[b)] Selectivity ratio = (IC_{50} of AChE)/(IC_{50} of BuChE).

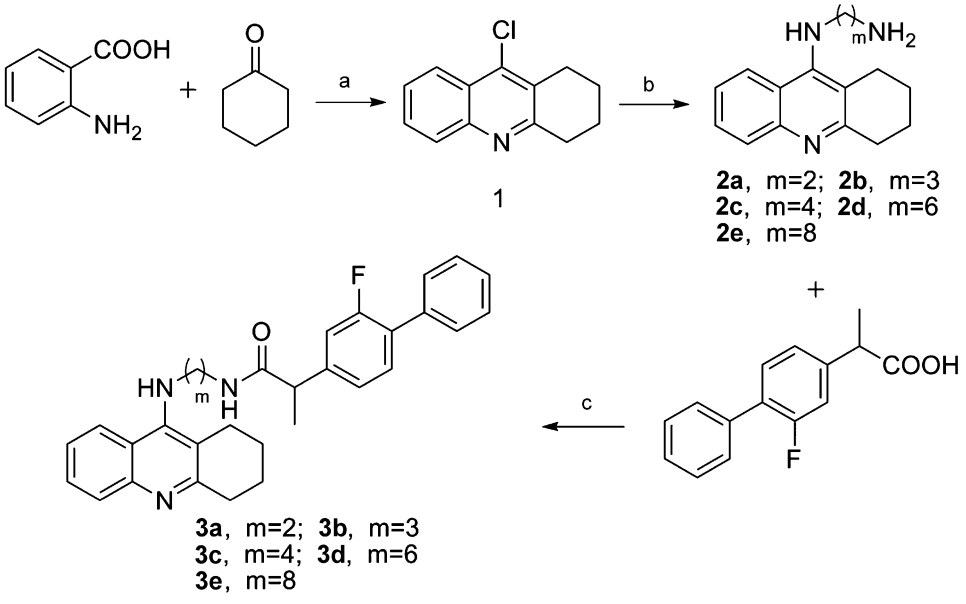

Scheme 1. General method for the synthesis of **3a–e**. Reagents: (a) $POCl_3$ reflux, 3 h; (b) pentanol $NH_2(CH_2)_mNH_2$, reflux, 18 h; and (c) DCC, DMAP, anhydrous CH_2Cl_2 room temp., 24 h.

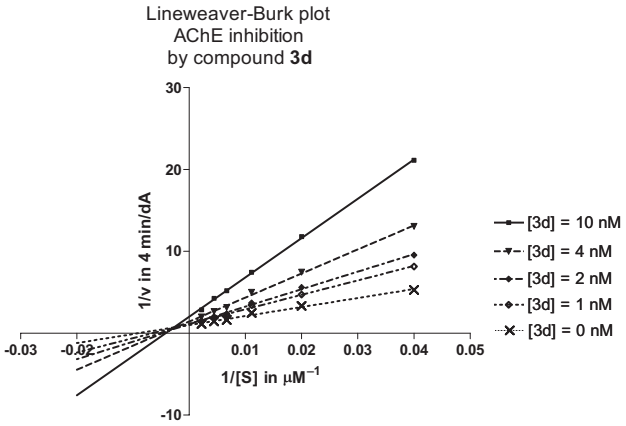

Figure 2. Lineweaver–Burk plots resulting from sub-velocity curves of AChE activity with different substrate concentrations (25–450 μM) in the absence and presence of 1, 2, 4, and 10 nM **3d**.

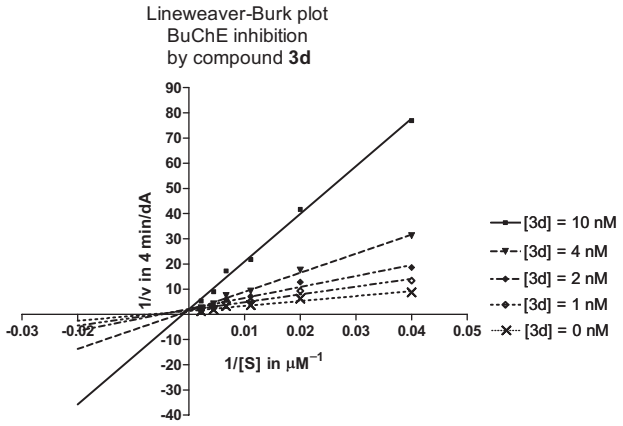

Figure 3. Lineweaver–Burk plots resulting from sub-velocity curves of BuChE activity with different substrate concentrations (25–450 μM) in the absence and presence of 1, 2, 4, and 10 nM **3d**.

Based on the good performance on both AChE and BuChE, **3d** was selected for kinetic measurements to study the binding mode of the novel compound. The mechanism was analyzed by Lineweaver–Burk reciprocal plots, which were reciprocal rates versus reciprocal substrate concentrations for different concentrations of **3d**. For AChE, the plot showed both increased slopes (decreased V_{max}) and intercepts (higher K_m) at increasing concentration of **3d** (Fig. 2), indicating a mixed-type inhibition. This demonstrates that the compound not only competes for the same catalytic active site (CAS) as the substrate ACh does, but also interacts with a second binding site. In contrast, a different plot for BuChE was observed, with different K_m and constant V_{max} at different concentrations of **3d** (Fig. 3). This suggested a competitive inhibition, indicating that this compound at this target competes orthosterically for the same binding site (CAS) as the substrate ACh does.

In order to further explore the binding mode of **3d** with AChE, a molecular modeling study using CDOCKER within Discovery Studio (DS, Accelrys) was performed (Fig. 4). As can be seen from the result, the binding conformation suggested that **3d** can cover the binding gorge in a satisfied orientation and mode, thus leading to the high inhibitory potency. The binding model also indicated that the tacrine fragment of **3d** was bound to near the bottom of the gorge (CAS) through strong parallel π–π stacking against the indole ring of Trp86. At the mouth of the gorge, the benzene ring of flurbiprofen group in **3d** showed hydrophobic interaction with the residues Tyr286, a key residue in the peripheral anionic site (PAS) [13], which is around 18 Å away from CAS and has been

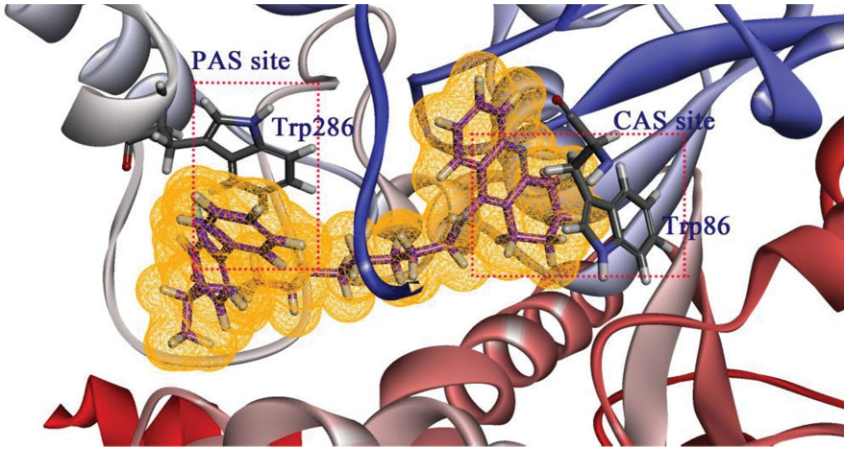

Figure 4. Representation of the binding mode of compound **3d** (purple) with AChE (PDB id: 2X8B).

proved to have close relation to the neurotoxic cascade of AD initiated by AChE-induced Aβ aggregation [14]. According to all the results, we postulated that compound **3d** might be a dual-binding site inhibitor of both PAS and CAS.

Before performing further pharmacology, toxicity was determined by using a 3-[4,5-dimethylthiazol-2-yl]-2,5-diphenyl-tetrazolium bromide (MTT) assay, and the result demonstrated that there was no significant toxicity when the concentration of **3d** was $<1\,\mu M$, which is beyond the concentration needed for significant effects in inhibiting CHEs and reducing the formation of $A\beta_{40}$.

To elucidate the potency of the compounds in inhibiting the formation of Aβ *in vitro*, the cell-based $A\beta_{40}$ reducing activity of compound **3d** was assessed by an enzyme-linked immune sandwich assay (ELISA) [15]. As can be seen from the result (Fig. 5), **3d** showed a significant 31% reduction of $A\beta_{40}$ formation at the concentration 0.25 μM, demonstrating that the target hybrid compound can inhibit the generation of Aβ, probably by inhibition of γ-secretase. However, reducing the production of β-amyloid affords much more higher concentration than inhibiting ChE activity. Flurbiprofen and tacrine did not show any Aβ reduction at this concentration.

In conclusion, we have designed and synthesized five novel tacrine–flurbiprofen hybrids **3a–e**. Two of the compounds (**3d** and **3e**) inhibit AChE more potently than tacrine and all compounds (except **3a**) exhibited better or the same BuChE inhibitory activity compared to tacrine. In addition, **3c** was found to be a significantly selective BuChE inhibitor. The inhibitory mechanism of **3d** was analyzed by Lineweaver–Burk reciprocal plots and docking and was recognized as a dual site (CAS and PAS) binding mode for AChE, whereas a competitive inhibition is performed for BuChE. Additionally, **3d** was chosen for the cell-based Aβ inhibition assay and showed significant potency in inhibiting the formation of $A\beta_{40}$. In recent years, several authors have postulated that neither the presence of monomeric nor polymeric but rather the accumulation of oligomeric β-amyloid causes the pathogenesis of Alzheimer disease. Nevertheless, in this study we looked at the inhibition of β-amyloid production because a lower level of the monomeric should also consequently reduce the quantity of oligomeric and polymeric aggregations of β-amyloid.

All the results characterized the novel tacrine–flurbiprofen hybrids as multi-potent anti-AD drug candidates, and **3d** might be a promising lead compound for further research.

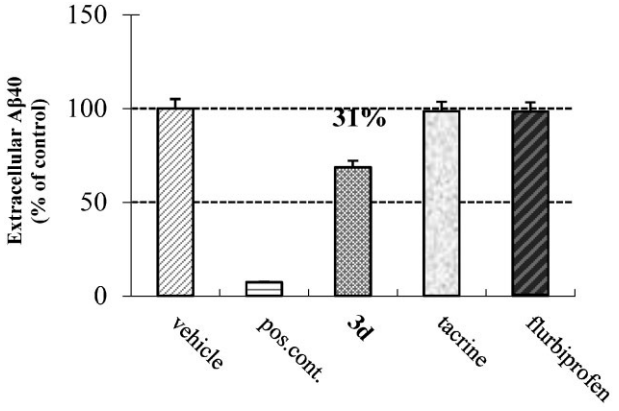

Figure 5. $A\beta_{40}$ reduction of **3d**, tacrine, and flurbiprofen (0.25 μM) in the cell-based assay. A known γ-secretase inhibitor, {1*S*-benzyl-4*R*-[1-(1*S*-carbamoyl-2-phenyl-ethyl-carbamoyl)-1*S*-3-methylbutyl-carbamoyl]-2*R*-hydrox-5-phenylpentyl}carbamic acid *tert*-butyl ester (L-685458), was used as a positive control.

Experimental

Chemistry

General methods

Melting points are uncorrected and were measured in open capillary tubes, using a Gallenkamp melting point apparatus. ^1H and ^{13}C NMR spectral data were obtained from a Bruker Advance 250 spectrometer (250 MHz). HRMS data were recorded using Agilent technologies LC/MSD TOF. TLC was performed on silica gel F254 plates (Merck). Column chromatography was carried out with silica gel 60, 63–200 μm (Baker). Elemental analyses were performed on a Heraeus Vario EL III apparatus (Firma Elementar Analysensysteme GmbH, Germany).

*9-Aminoalkylamino-1,2,3,4-tetrahydroacridines (**2a–e**) – General procedure I*

To a solution of **1** (9-chlorotetrahydroacridine) in 10 mL of pentanol 3 molar equiv. of diaminolkane were added. After refluxing for 18 h under nitrogen, the solution was cooled to 0°C and then acidified to pH 2 with HCl/ether solution. The deposit was separated and dissolved in 10 mL of water; then the solution was basified to pH 10 with a saturated aqueous solution of Na_2CO_3 and extracted with CH_2Cl_2 (3×10 mL). The combined organic layers were washed with brine, dried over anhydrous Na_2SO_4, and evaporated *in vacuo*. The residue was purified by column chromatography (CH_2Cl_2/MeOH = 7:3 v/v, plus 5 mL triethylamine per 1000 mL).

*9-(2-Aminoethylamino)-1,2,3,4-tetrahydroacridine (**2a**)*

Following general procedure I, using **1** (2.17 g, 10 mmol) and 1,2-diaminoethane (2.00 mL, 30 mmol). Brownish oil (1.45 g, 60%). ^1H NMR ($CDCl_3$): δ 8.02–7.99 (d, 1H, arom), 7.93–7.89 (d, 1H, arom), 7.58–7.51 (t, 1H, arom), 7.37–7.31 (t, 1H, arom), 4.83 (br, 1H, NHCH$_2$), 3.50–3.48 (t, 2H, NHCH$_2$), 3.06–3.03 (t, 2H, C4-H$_2$), 2.98–2.93 (m, 2H, CH$_2$NH$_2$), 2.80–2.76 (t, 2H, C1-H$_2$), 1.94–1.89 (m, 4H, C3-H$_2$, C2-H$_2$). HRMS (ESI) *m/z* calcd. for $C_{15}H_{19}N_3$ [M^+] 241.1579; found 241.1579.

*9-(3-Aminopropylamino)-1,2,3,4-tetrahydroacridine (**2b**)*

From **1** (2.17 g, 10 mmol) and 1,3-diaminopropane (2.49 mL, 30 mmol). Brownish oil (1.37 g, 54%). ^1H NMR ($CDCl_3$) δ 7.98–7.95 (d, 1H, arom), 7.89–7.86 (m, 1H, arom), 7.54–7.48 (t, 1H, arom), 7.33–7.27 (t, 1H, arom), 3.59–3.53 (t, 2H, NHCH$_2$), 3.03 (br, 2H,

C4-H_2), 2.88–2.83 (t, 2H, CH_2NH$_2$), 2.69 (br, 2H, C1-H_2), 1.89–1.87 (m, 4H, C3-H_2, C2-H_2), 1.83–1.71 (m, 2H, CH_2CH$_2$NH$_2$). HRMS (ESI) *m/z* calcd. for $C_{16}H_{21}N_3$ [M^+] 255.1735; found 255.1737.

*9-(4-Aminobutylamino)-1,2,3,4-tetrahydroacridine (**2c**)*

From **1** (2.17 g, 10 mmol) and 1,4-diaminobutane (3.01 mL, 30 mmol). Brownish oil (1.35 g, 50%). ^{1}H NMR ($CDCl_3$) δ 7.96–7.88 (m, 2H, arom), 7.57–7.51 (t, 1H, arom), 7.36–7.30 (t, 1H, arom), 3.52–3.46 (t, 2H, NHCH_2), 3.05 (br, 2H, C4-H_2), 2.75–2.70 (m, 4H, CH_2NH$_2$, C1-H_2), 1.92–1.89 (m, 4H, C3-H_2, C2-H_2), 1.76–1.64 (m, 2H, CH_2CH$_2$NH$_2$), 1.59–1.50 (m, 2H, NHCH$_2$CH_2). HRMS (ESI) *m/z* calcd. for $C_{17}H_{23}N_3$ [M^+] 269.1892; found 269.1892.

*9-(5-Aminopentylamino)-1,2,3,4-tetrahydroacridine (**2d**)*

From **1** (2.17 g, 10 mmol) and 1,6-diaminohexane (3.48 g, 30 mmol). Brownish oil (1.97 g, 66%). ^{1}H NMR ($CDCl_3$): δ 7.97–7.89 (m, 2H, arom), 7.58–7.51 (m, 1H, arom), 7.37–7.30 (m, 1H, arom), 3.97 (br, 1H, NHCH$_2$), 3.51–3.45 (m, 2H, NHCH_2), 3.06 (br, 2H, C4-H_2), 2.70–2.64 (m, 4H, CH_2NH$_2$, C1-H_2), 1.94–1.90 (m, 4H, C3-H_2, C2-H_2), 1.72–1.61 (m, 2H, NHCH$_2$CH_2), 1.47–1.37 (m, 6H, CH_2CH$_2$CH$_2$CH$_2$NH$_2$). HRMS (ESI) *m/z* calcd. for $C_{19}H_{27}N_3$ [M^+] 297.2205; found 297.2203.

*9-(8-Aminooctylamino)-1,2,3,4-tetrahydroacridine (**2e**)*

From **1** (2.17 g, 10 mmol) and 1,8-diaminooctane (4.32 g, 30 mmol). Brownish oil (1.52 g, 48%). ^{1}H NMR ($CDCl_3$): δ 7.95–7.86 (m, 2H, arom), 7.55–7.49 (m, 1H, arom), 7.34–7.28 (m, 1H, arom), 3.92 (br, 1H, NHCH$_2$), 3.47–3.42 (t, 2H, NHCH_2), 3.04 (br, 2H, C4-H_2), 2.68–2.61 (m, 4H, CH_2NH$_2$, C1-H_2), 1.94–1.88 (m, 4H, C3-H_2, C2-H_2), 1.65–1.57 (m, 2H, NHCH$_2$CH_2), 1.45–1.28 (m, 10H, CH_2CH_2CH_2CH_2CH_2CH$_2$NH$_2$). HRMS (ESI) *m/z* calcd. for $C_{21}H_{31}N_3$ [M^+] 325.2518; found 325.2518.

*2-(2-Fluorobiphenyl-4-yl)-N-[(1,2,3,4-tetrahydroacridin-9-ylamino)alkyl]propanamides (**3a–e**) – General procedure II*

Flurbiprofen and an equiv. molar amount of *N*,*N*′-dicyclohexylcarbodiimide (DCC) were dissolved in 20 mL of dry CH_2Cl_2 and the mixture was stirred at room temperature for 0.5 h. Then a solution of an equiv. molar amount of **2** in 5 mL of dry CH_2Cl_2 was added, followed by a catalytic amount of 4-dimethylaminopyridine (DMAP). After being stirred for 24 h at room temperature, the reaction was quenched by adding 10 mL of H_2O. Then the resulting mixture was filtrated and the filtrate was extracted with CH_2Cl_2 (3×15 mL). The combined organic phases were washed with brine, dried over anhydrous Na_2SO_4, and evaporated *in vacuo*. The residue was purified by column chromatography (CH_2Cl_2/MeOH = 10:1 v/v).

*2-(2-Fluorobiphenyl-4-yl)-N-[2-(1,2,3,4-tetrahydroacridin-9-ylamino)ethyl]propanamide (**3a**)*

Following general procedure I, compound **2a** (0.24 g, 1 mmol) reacted with flurbiprofen (0.24 g, 1 mmol) to furnish **3a** as a yellow solid (0.19 g, 41%); m.p. 76–78°C. ^{1}H NMR ($CDCl_3$): δ 7.89–7.84 (m, 2H, arom), 7.50–7.23 (m, 8H, arom), 7.10–7.06 (d, 2H, arom), 6.68–6.64 (t, 1H, NHCO), 4.74 (br, 1H, NH), 3.63–3.52 (m, 5H, NHCH_2CH_2, CHCH$_3$), 2.98 (br, 2H, C4-H_2), 2.61 (br, 2H, C1-H_2), 1.81 (br, 4H, C3-H_2, C2-H_2), 1.53–1.50 (d, 3H, CHCH_3); ^{13}C NMR ($CDCl_3$): δ 175.00 (NHCO), 161.70, 157.74 (arom, C^3), 158.15 (arom), 150.65 (arom), 146.80 (arom), 142.61, 142.48 (arom, C^1), 135.24 (arom, $C^{1'}$), 131.06, 130.99 (arom, C^5), 128.87 (arom, $C^{6'}$, $C^{2'}$), 128.81 (arom), 128.55 (arom), 128.47 (arom, $C^{3'}$, $C^{5'}$), 128.00, 127.75 (arom, C^4), 127.78 (arom, $C^{4'}$), 123.88 (arom), 123.58, 123.53 (arom, C^6), 122.58 (arom), 119.82 (arom), 116.07 (arom), 115.45, 115.07 (arom, C^2), 49.42 (NHCH$_2$), 46.40, 46.39 (CHCH$_3$), 40.72 (CH$_2$NHCO), 33.59 (C4), 24.98 (C1), 22.91 (C3), 22.58 (C2), 18.58 (CHCH$_3$). Anal. calcd. for ($C_{30}H_{30}FN_3O \cdot 1/2H_2O$): found C, 75.5; H, 6.52; N, 8.8; requires C, 75.6; H, 6.56; N, 8.8.

*2-(2-Fluorobiphenyl-4-yl)-N-[3-(1,2,3,4-tetrahydroacridin-9-ylamino)propyl]propanamide (**3b**)*

Compound **2b** (0.26 g, 1 mmol) reacted with flurbiprofen (0.24 g, 1 mmol) to furnish **3b** as a yellow solid (0.21 g, 43%); m.p. 67–69°C. ^{1}H NMR ($CDCl_3$): δ 7.97–7.87 (m, 2H, arom), 7.55–7.29 (m, 8H, arom), 7.13–7.08 (m, 2H, arom), 6.22–6.18 (t, 1H, NHCO), 4.63 (br, 1H, NH), 3.64–3.55 (q, 1H, CHCH$_3$), 3.42–3.40 (m, 4H, NHCH_2CH$_2$CH_2), 3.02–2.98 (m, 2H, C4-H_2), 2.71 (br, 2H, C1-H_2), 1.86 (br, 4H, C3-H_2, C2-H_2), 1.80–1.70 (m, 2H, NHCH$_2$CH_2), 1.57–1.54 (d, 3H, CHCH_3); ^{13}C NMR ($CDCl_3$): δ 174.34 (NHCO), 161.73, 157.77 (arom, C^3), 158.44 (arom), 150.63 (arom), 147.08 (arom), 142.68, 142.56 (arom, C^1), 135.20 (arom, $C^{1'}$), 131.03, 130.96 (arom, C^5), 128.84 (arom, $C^{6'}$, $C^{2'}$), 128.79 (arom), 128.45 (arom, $C^{3'}$, $C^{5'}$), 128.40 (arom), 127.97, 127.75 (arom, C^4, $C^{4'}$), 123.93 (arom), 123.60, 123.54 (arom, C^6), 122.56 (arom), 120.41 (arom), 116.82 (arom), 115.46, 115.09 (arom, C^2), 46.59 (CHCH$_3$), 45.69 (NHCH$_2$), 37.07 (CH$_2$NHCO), 33.82 (C4), 31.26 (NHCH$_2$CH_2), 24.99 (C1), 22.98 (C3), 22.68 (C2), 18.57 (CHCH$_3$). Anal. calcd. for ($C_{31}H_{32}FN_3O \cdot 1/2H_2O$): found C, 75.6; H, 6.63; N, 8.7; requires C, 75.9; H, 6.78; N, 8.6.

*2-(2-Fluorobiphenyl-4-yl)-N-[4-(1,2,3,4-tetrahydroacridin-9-ylamino)butyl]propanamide (**3c**)*

Compound **2c** (0.27 g, 1 mmol) reacted with flurbiprofen (0.24 g, 1 mmol) to furnish **3c** as a yellow solid (0.23 g, 46%); m.p. 63–65°C. ^{1}H NMR ($CDCl_3$): δ 7.94–7.91 (d, 2H, arom), 7.55–7.31 (m, 8H, arom), 7.14–7.09 (m, 2H, arom), 6.22–6.18 (t, 1H, NHCO), 4.31 (br, 1H, NH), 3.64–3.49 (m, 3H, CHCH$_3$, NHCH_2), 3.30–3.23 (m, 2H, CH_2NHCO), 3.02 (br, 2H, C4-H_2), 2.63 (br, 2H, C1-H_2), 1.85 (br, 4H, C3-H_2, C2-H_2), 1.66–1.49 (m, 7H, NHCH$_2$CH_2CH_2, CHCH_3); ^{13}C NMR ($CDCl_3$): δ 173.76 (NHCO), 161.69, 157.42 (arom, C^3), 157.74 (arom), 151.20 (arom), 146.13 (arom), 143.04, 142.92 (arom, C^1), 135.31 (arom, $C^{1'}$), 130.93, 130.87 (arom, C^5), 128.86 (arom, $C^{6'}$, $C^{2'}$), 128.81 (arom), 128.45 (arom, $C^{3'}$, $C^{5'}$), 127.81, 127.60 (arom, C^4), 127.71 (arom), 127.39, (arom, $C^{4'}$), 123.92 (arom), 123.60, 123.54 (arom, C^6), 122.94 (arom), 119.63 (arom), 115.49 (arom), 115.42, 115.04 (arom, C^2), 48.66 (NHCH$_2$), 46.43 (CHCH$_3$), 39.16 (CH$_2$NHCO), 33.17 (C4), 28.73 (CH$_2$CH$_2$NHCO), 26.99 (C1), 24.67 (NHCH$_2$CH_2), 22.81 (C3), 22.41 (C2), 18.56 (CHCH$_3$). Anal. calcd. for ($C_{32}H_{34}FN_3O \cdot H_2O$): found C, 74.8; H, 6.87; N, 8.0; requires C, 74.8; H, 7.06; N, 8.2.

*2-(2-Fluorobiphenyl-4-yl)-N-[6-(1,2,3,4-tetrahydroacridin-9-ylamino)hexyl]propanamide (**3d**)*

Compound **2d** (0.30 g, 1 mmol) reacted with flurbiprofen (0.24 g, 1 mmol) to furnish **3d** as a yellow solid (0.23 g, 44%); m.p. 57–59°C. ^{1}H NMR ($CDCl_3$): δ 8.01–7.97 (m, 2H, arom), 7.57–7.52 (m, 3H, arom), 7.48–7.30 (m, 5H, arom), 7.17–7.10 (m, 2H, arom), 5.98–5.94 (t, 1H, NHCO), 4.44 (br, 1H, NH), 3.64–3.48 (m, 3H, CHCH$_3$, NHCH_2), 3.26–3.18 (m, 2H, CH_2NHCO), 3.07 (br, 2H, C4-H_2), 2.65 (br, 2H, C1-H_2), 1.88 (br, 4H, C3-H_2, C2-H_2), 1.68–1.57 (m, 2H, NHCH$_2$CH_2), 1.53–1.25 (m, 9H, CH_2CH_2CH_2CH$_2$NHCO,

$CHC\underline{H}_3$); ^{13}C NMR ($CDCl_3$): δ 173.57 ($NH\underline{C}O$), 161.69, 156.92 (arom, C^3), 157.74 (arom), 151.69 (arom), 145.65 (arom), 143.14, 143.02 (arom, C^1), 135.34 (arom, $C^{1'}$), 130.91, 130.85 (arom, C^5), 128.86 (arom), 128.81 (arom, $C^{6'}$, $C^{2'}$), 128.45 (arom, $C^{3'}$, $C^{5'}$), 127.78, 127.56 (arom, C^4), 127.69 (arom), 127.00 (arom, $C^{4'}$), 123.89 (arom), 123.63, 123.58 (arom, C^6), 123.15 (arom), 119.29 (arom), 115.41 (arom), 115.04, 114.84 (arom, C^2), 48.93 ($NH\underline{C}H_2$), 46.48 ($\underline{C}HCH_3$), 39.33 ($\underline{C}H_2NHCO$), 32.85 ($NHCH_2\underline{C}H_2$), 31.40 ($\underline{C}H_2CH_2NHCO$), 29.39 (C4), 26.32 ($NHCH_2CH_2\underline{C}H_2$), 26.29 (C1), 24.56 ($\underline{C}H_2CH_2CH_2NHCO$), 22.79 (C3), 22.32 (C2), 18.56 ($CH\underline{C}H_3$). Anal. calcd. for ($C_{34}H_{38}FN_3O\cdot H_2O$): found C, 75.6; H, 7.21; N, 7.8; requires C, 75.4; H, 7.44; N, 7.8.

*2-(2-Fluorobiphenyl-4-yl)-N-[8-(1,2,3,4-tetrahydroacridin-9-ylamino)octyl]propanamide (**3e**)*

Compound **2e** (0.31 g, 1 mmol) reacted with flurbiprofen (0.24 g, 1 mmol) to furnish **3e** as a yellow solid (0.22 g, 40%); m.p. 50–52°C. ^1H NMR ($CDCl_3$): δ 7.96–7.89 (t, 2H, arom), 7.56–7.50 (m, 3H, arom), 7.44–7.30 (m, 5H, arom), 7.15–7.09 (t, 2H, arom), 5.78 (br, 1H, $N\underline{H}CO$), 3.99 (br, 1H, $N\underline{H}$), 3.60–3.41 (m, 3H, $C\underline{H}CH_3$, $NHC\underline{H}_2$), 3.24–3.16 (m, 2H, $C\underline{H}_2NHCO$), 3.05 (br, 2H, C4-H_2), 2.68 (br, 2H, C1-H_2), 1.90 (br, 4H, C3-H_2, C2-H_2), 1.64–1.51 (m, 5H, $NHCH_2C\underline{H}_2$, $CHC\underline{H}_3$), 1.44–1.24 (m, 10H, $C\underline{H}_2C\underline{H}_2C\underline{H}_2C\underline{H}_2C\underline{H}_2CH_2NHCO$); ^{13}C NMR ($CDCl_3$): δ 173.39 ($NH\underline{C}O$), 161.72, 157.77 (arom, C^3), 158.22 (arom), 150.93 (arom), 147.22 (arom), 143.11, 143.00 (arom, C^1), 135.39 (arom, $C^{1'}$), 130.95, 130.89 (arom, C^5), 128.88 (arom), 128.84 (arom, $C^{6'}$, $C^{2'}$), 128.45 (arom, $C^{3'}$, $C^{5'}$), 128.37 (arom), 127.82, 127.60 (arom, C^4), 127.69 (arom, $C^{4'}$), 123.60 (arom), 123.60, 123.55 (arom, C^6), 122.92 (arom), 120.08 (arom), 115.66 (arom), 115.42, 115.04 (arom, C^2), 49.38 ($NH\underline{C}H_2$), 46.61, 46.59 ($\underline{C}HCH_3$), 39.63 ($\underline{C}H_2NHCO$), 33.87 ($NHCH_2\underline{C}H_2$), 31.68 ($\underline{C}H_2CH_2NHCO$), 29.44 ($NHCH_2CH_2CH_2\underline{C}H_2$), 29.15 ($\underline{C}H_2CH_2CH_2CH_2NHCO$), 29.03 (C4), 26.75 ($NHCH_2CH_2\underline{C}H_2$), 26.63 ($\underline{C}H_2CH_2CH_2NHCO$), 24.73 (C1), 23.01 (C3), 22.72 (C2), 18.60 ($CH\underline{C}H_3$). Anal. calcd. for ($C_{36}H_{42}FN_3O\cdot 3/4H_2O$): found C, 76.6; H, 7.67; N, 7.3; requires C, 76.5; H, 7.76; N, 7.4.

Pharmacology

Cholinesterase inhibition assay in vitro

The assay followed the method of Ellman et al., using a Shimadzu 160 Spectrophotometer. AChE (E.C.3.1.1.7, Type VI-S, from electric eel) and BChE (E.C.3.1.1.8, from equine serum), 5,5′-dithiobis(2-nitrobenzoic acid) (Ellman's reagent, DTNB), acetylthiocholine (ATC), and butyrylthiocholine (BTC) iodides were purchased from Sigma–Aldrich (Steinheim, Germany). AChE/BChE stock solution was prepared by adjusting 500 units of the enzyme and 1 mL of gelatine solution (1% in water) to 100 mL with water. This enzyme solution was further diluted before use, to give 2.5 units/mL in 1.4 mL aliquots. 0.075 M ATC/BTC iodide solution was prepared in water. 0.01 M DTNB solution was prepared in water containing 0.15% w/v sodium bicarbonate. For buffer preparation, potassium dihydrogen phosphate (1.36 g, 10 mmol) was dissolved in 100 mL of water and adjusted with KOH to pH 8.0 ± 0.1. Stock solutions of the test compounds were prepared in ethanol, 100 μL of which gave a final concentration of 10^{-4} M when diluted to the final volume of 3.32 mL. For each compound, a dilution series of at least five different concentrations (normally 10^{-4}–10^{-9} M) were prepared.

For measurement, a cuvette containing 3.0 mL of phosphate buffer, 100 μL of the respective enzyme, and 100 μL of the test compound solution was allowed to stand for 5 min before 100 μL of DTNB was added. The reaction was started by addition of 20 μL of the substrate solution (ATC/BTC). The solution was mixed immediately, and exactly 2 min after substrate addition, the absorption was measured at 25°C at 412 nm. For the reference value, 100 μL of water replaced the test compound solution. For determining the blank value, additionally 100 μL of water replaced the enzyme solution. Each concentration was measured in triplicate at 25°C. The inhibition curve was obtained by plotting percentage enzyme activity (100% for the reference) versus logarithm of test compound concentration. Calculation of the IC_{50} values was performed with Graph Pad Prism™ 4.

Kinetic measurements were performed in the same manner, while the substrate (ATC/BTC) was used in concentrations of 25, 50, 90, 150, 226, and 452 μM for each test compound concentration and the reaction was extended to 4 min before measurement of the absorption. V_{max} and K_m values of the Michaelis–Menten kinetics were calculated by nonlinear regression from substrate–velocity curves using Graph Pad Prism™ 4. Linear regression was used for calculating the Lineweaver–Burk plots.

Cell-based Aβ inhibition assay

$A\beta_{40}$ were measured in culture medium of primary cortical neuron cells (pregnant Wistar rats). Cells were seeded onto 48-well plates and allowed to grow for 3–5 days in 5% CO_2/95% air in a humidified atmosphere. Cells were incubated for 24 h with test compound at concentration 0.25 μM. {1*S*-Benzyl-4*R*-[1-(1*S*-carbamoyl-2-phenyl-ethyl-carbamoyl)-1*S*-3-methylbutylcarbamoyl]-2*R*-hydrox-5-phenylpentyl}carbamic acid *tert*-butyl ester (L-685458) was used as positive control. DMSO (0.3%) was used as negative control. Following incubation with the test compounds the supernatant was collected and the $A\beta_{40}$ levels were determined using a sandwich human/rat β-amyloid (40) ELISA kit II, performed in 96-well microtiter plates. Conditioned media was incubated with capture antibody for 16 h at 4°C, followed by washing. The detecting antibody incubation was performed for 2 h at 4°C, again followed by the wash steps. Then, 100 μL of TMB ultrasubstrate was added and incubated for 30 min at room temperature in the dark, and the reaction was stopped by adding 100 μL of 2 M H_2SO_4. Absorbance at 450 nm was recorded with a Microplate Reader TECAN Safire2 (Tecan Group Ltd., Maennedorf, Switzerland). $A\beta_{40}$ was used to generate standard curves. The percent of control $A\beta_{40}$ as a function of the concentration of the test compound was recorded. Triplicate measurements from each drug concentration were averaged.

The cytotoxicity potential of test compound was assessed in the same cells of the Aβ assay using the 3-[4,5-dimethylthiazol-2-yl]-2,5-diphenyltetrazolium bromide (MTT) assay. After adding increasing concentrations of test compound (ranging from 0.01 to 100 μM), cells were incubated for 24 h. Then cells with 100 μL of culture medium containing 20μL (0.5 mg/mL) of MTT were incubated for another 4 h at 37°C, 5% CO_2, and saturated humidity. After removal of the medium, an amount of 120 μL of 100% DMSO was added to each well. The amount of formed formazan was determined by reading the samples at 570 nm.

Molecular docking

The docking study was performed by using CDOCKER module inbuilt in Discovery Studion 3.0. In general, CDOCKER generated ligand "seeds" to populate the binding pocket. Each seed was then subjected to high-temperature molecular dynamics (MD) using a

modified version of CHARMm force field. Each of the structures from the MD run were then located and fully minimized. The solutions were then clustered according to position and conformation and ranked by energy. CHARMm charges were used for the protein structure. The crystal structure of human AChE (HuAChE, PDB id: 2 × 8B) was selected for molecular docking. As there was no small molecule binding to 2 × 8B, the co-crystal structure of bis(7)-tacrine with TcAChE (PDB id: 2CKM) was selected as the reference structure. The 2 × 8B was firstly aligned and superimposed onto the 2CKM (see Supporting Information Fig. S1). The RMSD between the two structures was 1.202. Additionally, the CAS site and the PAS site of the two kinds of AChE exhibit high similarity, indicating that the reference structure is reliable in this study. After the superimposition, the residues around bis(7)-tacrine in HuAChE (in 10 Å radius) was set as binding site. For CDOCKER simulation, the heating step, cooling steps, and cooling temperature were set to 5000, 10,000, and 310, respectively. Other parameters were kept as default.

The support by "DAAD Sandwich Program" Scholarship (April 2010 to March 2012) for Chen Yao is very gratefully acknowledged. The authors also thank National Science Foundation of China (NSFC, No. 30973608), National Natural Science Foundation of China (No. 81070967), and the Natural Science Foundation of Jiangsu Province of China (No. BK2009296) for further funding.

The authors have declared no conflict of interest.

References

[1] H. W. Querfurth, F. M. LaFerla, N. Engl, *J. Med.* **2010**, *362*, 329–344.

[2] E. Scarpini, P. Scheltens, H. Feldman, *Lancet Neurol.* **2003**, *2*, 539–547.

[3] U. Holzgrabe, P. Kapková, V. Alptüzün, J. Scheiber, E. Kugelmann, *Expert Opin. Ther. Targets* **2007**, *11*, 161–179.

[4] C. G. Ballard, *Eur. Neurol.* **2002**, *47*, 64–70.

[5] J. Hardy, D. J. Selkoe, *Science* **2002**, *297*, 353–356.

[6] R. Vassar, D. M. Kovacs, R. Yan, P. C. Wong, *J. Neurosci.* **2009**, *29*, 12787–12794.

[7] I. Peretto, S. Radaelli, C. Parini, M. Zandi, L. F. Raveglia, G. Dondio, L. Fontanella, P. Misiano, C. Bigogno, A. Rizzi, B. Riccardi, M. Biscaioli, S. Marchetti, P. Puccini, S. Catinella, I. Rondelli, V. Cenacchi, P. T. Bolzoni, P. Caruso, G. Villetti, F. Facchinetti, E. D. Giudice, N. Moretto, B. P. Imbimbo, *J. Med. Chem.* **2005**, *48*, 5705–5720.

[8] M. B. Youdim, J. J. Buccafusso, *Trends Pharmacol. Sci.* **2005**, *26*, 27–35.

[9] L. Fang, B. Kraus, J. Lehmann, J. Heilmann, Y. H. Zhang, M. Decker, *Bioorg. Med. Chem. Lett.* **2008**, *18*, 2905–2909.

[10] M. I. Fernández-Bachiller, C. Pérez, G. C. González-Muñoz, S. Conde, M. G. López, M. Villarroya, A. G. García, M. S. Rodríguez-Franco, *J. Med. Chem.* **2010**, *53*, 4927–4937.

[11] P. R. Carlier, Y. F. Han, E. S.-H. Chow, C. P.-L. Li, H. Wang, T. X. Lieu, H. S. Wong, Y.-P. Pang, *Bioorg. Med. Chem.* **1999**, *7*, 351–357.

[12] G. L. Ellman, K. D. Courtney, V. Andres, Jr., R. M. Feather-Stone, *Biochem. Pharmacol.* **1961**, *7*, 88–95.

[13] Y. Bourne, P. Taylor, Z. Radi , P. Marchot, *EMBO J.* **2003**, *22*, 1–12.

[14] M. Bartolini, C. Bertucci, V. Cavrini, V. Andrisano, *Biochem. Pharmacol.* **2003**, *65*, 407–416.

[15] T. H. Al-Tel, M. H. Semreen, R. A. Al-Qawasmeh, M. F. Schmidt, R. El-Awadi, M. Ardah, R. Zaarour, S. N. Rao, O. El-Agnaf, *J. Med. Chem.* **2011**, *54*, 8373–8385.

